HHS Public Access

Author manuscript

*ACS Nano*. Author manuscript; available in PMC 2020 April 23.

Published in final edited form as:

*ACS Nano*. 2019 April 23; 13(4): 3783–3795. doi:10.1021/acsnano.9b01034.

# Optical Nano-Printing of Colloidal Particles and Functional Structures

**Jingang Li**[1,#], **Eric H. Hill**[2,#], **Linhan Lin**[1], and **Yuebing Zheng**[1,*]

[1]Department of Mechanical Engineering, Materials Science & Engineering Program and Texas Materials Institute, The University of Texas at Austin, Austin, Texas 78712, United States

[2]Institute of Advanced Ceramics, Hamburg University of Technology, 21073 Hamburg, Germany

## Abstract

Recent advances in chemical sciences have enabled the tailorable synthesis of colloidal particles with variable composition, size, shape and properties. Building superstructures with colloidal particles as building blocks is appealing for the fabrication of functional metamaterials and nanodevices. Optical nano-printing provides a versatile platform to print various particles into arbitrary configurations with nanometric precision. In this review, we summarize recent progress in optical nano-printing of colloidal particles and its related applications. Diverse techniques based on different physical mechanisms, including optical forces, light-controlled electric fields, optothermal effects, laser-directed thermo-capillary flows, and photochemical reactions, are discussed in detail. With its flexible and versatile capabilities, optical nano-printing will find promising applications in numerous fields such as nanophotonics, energy, microelectronics, and nanomedicine.

## Graphical Abstract

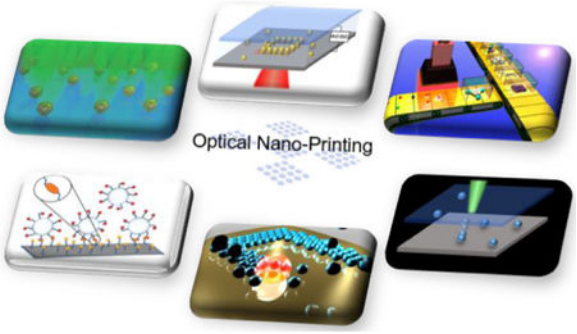


### Keywords

optical printing; colloidal particles; lasers; optical forces; optomechanical coupling; optoelectric fields; optothermal effect; photochemical reactions; colloidal nanostructures

[*]**Corresponding Author** zheng@austin.utexas.edu.

[#]J.L. and E.H.H. contributed equally to this work.

Nanofabrication is the core technique in modern nanotechnology to effectively manufacture various functional devices with a wide range of applications. Conventional top-down methods like electron-beam lithography and focused ion-beam lithography can produce nanostructures with precise size and shape control. However, such methods suffer from small sample volume, high cost, and complex instrumentation.[1] In addition, lithographic techniques are inherently limited to planar geometries and single-component structures.

Recently, colloidal particles have provided an appealing platform to construct nanostructures. Chemical synthesis permits the production of colloidal particles with precisely tunable sizes and shapes, tailorable compositions, and intriguing properties.[2-5] The perfection of atomic-scale crystallinity also permits high-quality devices with minimum material defects.[6-8] Self-assembly provides a low-cost way to autonomously build colloidal particles into large-scale patterns.[9] Nevertheless, it is restricted to thermodynamically stable colloidal structures and precise control is challenging. By combining top-down fabrication and self-assembly approaches, templated-assisted self-assembly has been developed to create various functional structures with accurate design.[10-13]

Optical nano-printing is an alternative strategy to construct superstructures using individual colloidal particles as building blocks.[14-16] Optical printing, the use of light to direct the formation of a desired image, has been of significant interest since the introduction of the first laser printers in the late 1960s.[17] Laser printing harnesses the ability of light to change the surface charge of the imaging drum, where the regions that have been exposed to the laser are without charge. Toner particles with negative charges are repelled by the imaging drum at the regions without laser exposure. Thus, toner can only be applied in the laser exposed areas, allowing the transfer of toner from the imaging drum to paper with predesigned patterns. In the 50 years since the introduction of laser printing, optical printing technology has developed far beyond its roots in office appliances, spawning a multitude of scientific applications. Compared to other nanofabrication techniques, optical nano-printing has great potential for the on-demand and site-specific construction of multi-component nanostructures. Using diverse colloidal particles as inks, optical nano-printing allows fabrication of multi-functional nanostructures for various nanotechnological applications such as optical metamaterials,[18, 19] photonic devices,[20, 21] and drug delivery.[22, 23] Moreover, the investigation of optical printing will provide an improved understanding of the physics of particle deposition[24, 25] and further our insights on light-matter interactions.[26-28]

In this article, we review the state-of-the-art optical nano-printing of colloidal particles achieved by different physical mechanisms (Figure 1). First, the optical forces exerted on the colloidal particles can be used to trap and deliver them to the substrate at single-particle resolution with high precision.[29-31] Apart from direct optical forces, indirect optomechanical coupling under a light-controlled electric or temperature field provides an alternative strategy to achieve manipulation and printing of colloidal particles. For example, laser illumination on photosensitive substrates induces local conductivity changes, and the electrophoretic or dielectrophoretic forces in the resulting electric field can drive particles to predesignated areas of the substrate.[32-36] Additionally, the entropically favorable photon-phonon conversion in optothermally responsive materials enables the generation of a strong temperature gradient field with low-power optical heating.[37, 38] By exploiting the

thermophoresis of colloidal species or thermo-capillary Marangoni flow,[39-42] one can achieve rational manipulation of colloidal particles in suspension. Optical heating also enables the transfer/release of nanoparticles from a donor substrate to a receiving substrate. Next, photochemical reactions offer additional possibilities for light-controlled patterning of chemically functionalized nanoparticles.[43] Finally, we summarize the challenges and prospects of optical nano-printing techniques for potential applications in a variety of scientific fields.

## OPTICAL NANO-PRINTING TECHNIQUES

In this section, we discuss current techniques in optical nano-printing based on different physical mechanisms. Optical printing based on optical forces is first introduced, with emphasis on plasmon-enhanced optical forces. Then, we describe the indirect optical printing of colloidal particles with a light-controlled optoelectric field, opto-thermophoretic effects, opto-thermomechanical strategies, and laser-generated microbubbles. Finally, immobilization and patterning of colloidal particles based on photochemical reactions are presented.

### Optical Forces.

Optical tweezers, which use optical gradient forces to trap colloidal particles, have been extensively applied for trapping and manipulation of dielectric particles, plasmonic particles, cells, and bacteria.[44-48] Laser patterning of nanoparticles using optical tweezers to trap and drive particles to desired positions has been demonstrated.[49-52] However, the laser wavelength in these cases is nonresonant with the localized surface plasmon resonance of the particles and additional steps or pretreatment of the colloidal dispersions are required to fix the particles to the substrate. For instance, gold nanoparticles (AuNPs) could be fixed to a glass substrate by ultraviolet (UV) laser irradiation, due to transient melting of AuNPs.[50]

Alternatively, Feldmann and coworkers reported direct optical printing of single AuNPs with a resonant laser (Figure 2A).[14] Both the AuNPs and the substrate are functionalized to have the same surface charge, which avoids the spontaneous deposition of AuNPs. When the incoming laser is of a similar wavelength as the localized surface plasmon resonances of the particles, the enhanced interaction between AuNPs and light gives rise to plasmon-enhanced optical forces. Figure 2B shows the calculated radial (left) and axial (right) optical forces acting on an 80 nm AuNP in a focused Gaussian beam. AuNPs illuminated by the laser are drawn toward the beam center by the radial force and pushed down toward the substrate by the axial force. Laser printing happens when the optical forces surpass the electrostatic repulsion between charged particle and substrate to enable the immobilization of AuNPs on the substrate by van der Waals interactions. By optimizing the wavelength and the optical power of the laser, single 100 nm AuNPs could be precisely printed on the target position with an accuracy of 50 nm. Arbitrary patterns can be formed by printing nanoparticles one by one, and the printed NPs can resist repeated cleaning and rinsing due to strong van der Waals forces (Figure 2C).[14] Throughput can be further increased by using a spatial light modulator to split a laser beam into several beams for patterning of multiple particles in

parallel (Figure 2D).[53] Rapid and precise fabrication of patterns with different shapes, sizes, and materials was realized in this way without the need for a photomask (Figure 2E).[53]

Plasmon-enhanced optical forces also offer added possibilities due to the need to overlap the laser wavelength with the localized surface plasmon resonance of the particle. Scherer and coworkers demonstrated plasmon-selective deposition of bipyramidal AuNPs using a near-infrared laser, while nonresonant spheroidal AuNPs could not be printed.[54] Two-color printing using two different laser wavelengths was developed to achieve orientation control of printed gold nanorods (AuNRs) (Figure 3A).[55] The laser that is nonresonant to the plasmon resonances of the nanorods is used to trap and align individual AuNRs, and another resonant laser is used to rapidly print the AuNRs at desired locations once the nanorods are aligned. This two-color approach enables fast printing and orientation control of AuNRs with an angular precision of ±16°. For instance, a printed “OX” pattern composed of perpendicularly-oriented AuNRs is shown in Figure 3B.

Laser printing had long been limited to the patterning of arrays composed of isolated plasmonic nanoparticles, as the achievable minimum inter-particle distance was restricted to ~300 nm.[28, 56] Recently, Stefani and coworkers proposed that this lateral resolution issue is a consequence of light absorption by the previously printed metallic nanoparticle, which generates large temperature gradients and the resulting photothermal repulsive forces prevent close printing of the second nanoparticle (Figure 3F).[57, 58] One strategy to avoid light absorption of the printed metal nanoparticle is to print another metal nanoparticle using a second laser wavelength at which the printed nanoparticle is transparent (Figure 3C).[57] In this way, sequential printing of the nanoparticles can take place uninterrupted. As a demonstration, Ag-Au heterodimers with various interparticle distances were fabricated (Figure 3D), and good orientation control over the connected heterodimers was shown (Figure 3E). Another strategy for reducing the minimum inter-particle distance is to optimize heat dissipation to reduce the photothermal repulsive forces.[58] Using a reduced graphene oxide coated sapphire substrate, optical printing of Au-Au nanoparticle dimers was successfully demonstrated (Figure 3G and Figure 3H). This capability is ascribed to a heat-sink effect due to the high thermal conductivity of reduced graphene oxide.[59,60]

Additionally, the high transient power density of femtosecond laser enables direct optical printing of colloidal nanoparticles. Sun and coworkers reported a femtosecond laser direct writing method for controlled assembly and patterning of metal nanostructures.[61, 62] Optical gradient forces drive the metal nanoparticles onto the substrate, which are then immobilized by van der Waals interactions.[62] Besides metal nanoparticles, this method can also be used for programmable fabrication of semiconductor quantum dot (QD) nanostructures with a resolution of ~170 nm.[63] Further discussions on femtosecond laser direct writing can be found in two recent reviews.[64, 65]

The use of optical forces offers a simple solution to directly print nanoparticles that strongly interact with light. Apart from plasmonic nanoparticles, the use of optical forces to print silicon nanoparticles has recently been demonstrated.[66] The capability to optically print connected metallic dimers further permits the fabrication of plasmonically coupled structures as well as functional devices. Furthermore, optical stamping strategies using a

spatial light modulator can greatly enhance the printing throughput, which is necessary to compete with more established and scalable techniques such as photolithography. However, a well-focused laser beam and complex optics are usually required for laser printing experiments. Pulsed lasers have the potential to extend the capabilities of laser printing, nevertheless, the high working power could damage fragile nanoparticles, biological components, and cells.[22, 67]

### Optoelectronic Printing.

In this section, we discuss optical printing by harnessing electrokinetic forces under a light-controlled electric field. Optoelectronic tweezers utilize both light and an alternate current (AC) electric bias to sculpt a potential landscape on a photosensitive substrate.[32, 33] Light illumination on a photosensitive substrate generates electron-hole pairs and increases the conductivity in the illuminated area to create “virtual electrodes” that locally concentrate the electric field. The resulting non-uniform electric field exerts a dielectrophoretic (DEP) force $F_{\mathrm{DEP}}$ on particles through the interaction of the induced dipole moments in particles and the surrounding media:

$$F_{\mathrm{DEP}} = 2\pi r^3 \varepsilon_m \alpha \nabla E^2 \quad (1)$$

where $r$ is the particle radius, $\varepsilon_m$ is the absolute permittivity of the surrounding medium, $\alpha$ is a parameter defining the effective polarizability of the particle, and $\nabla E^2$ is proportional to the gradient and the strength of the non-uniform electric field.[68]

DEP forces have been widely applied for trapping, manipulation, assembly, and sorting of particles and molecules.[34, 69-73] Wu and coworkers developed an optoelectronic platform for dynamic light-actuated printing of nanoparticles, dubbed NanoPen.[74] An optical pattern is projected onto a photosensitive hydrogenated amorphous silicon (a-Si:H) layer to create a non-uniform electric field under an AC bias, generating DEP forces acting on the nanoparticles. In addition to DEP forces, the non-uniform electric field and the heat generated by light absorption of the a-Si:H layer result in two other electrokinetic forces: light-actuated electroosmotic flow and electrothermal flow. Both the electroosmotic flow and the electrothermal flow contribute to the long-range flow-based collection of particles, while the DEP forces lead to the short-range attraction and immobilization of nanoparticles at the illuminated area (Figure 4A). The combination of these electrokinetic forces provides a versatile tool for low-power and high-throughput printing of large-area patterns (Figure 4B). Furthermore, the linewidth and density of immobilized structures can be controlled by tuning the AC voltage source parameters (*e.g.*, peak-to-peak voltage and frequency), light source parameters (*e.g.*, optical intensity and beam size), and operational parameters (*e.g.*, exposure time and scanning speed).

Apart from AC electric field-induced dielectrophoresis, electrophoresis based on direct current (DC) electric fields can also be exploited for optical printing applications.[75] Pascall *et al.* demonstrated light-directed electrophoretic deposition using light and DC electric fields to dynamically fabricate multi-material composites with arbitrary 3D patterns on

photoconductive electrodes.[76] Recently, optoelectric printing of plasmonic nanoparticles into arbitrary 2D circuits using laser and DC electric field was reported.[77] A laser beam is focused on an indium tin oxide substrate to create a laser-heated region working as a light-activated "virtual electrode". In the presence of a uniform electric field, nanoparticles can be massively captured and printed onto the substrate along the laser exposed area (Figure 4C). Unlike NanoPen, this method does not require the use of a photoconductive substrate or a high-frequency AC electric field. Tailored deposition of plasmonic nanoparticles can be achieved by simply reconfiguring the shape of the laser curve and controlling the printing time. The printed plasmonic nanoparticle assemblies are promising for tunable light scatterers at the micro-/nano-scale and biosensing applications (Figure 4D).

Light-driven deposition of colloidal particles with the assistance of AC/DC electric fields enables fast printing of large-area patterns, and arbitrary structures can be fabricated by shaping the projected light curve on the targeted substrate. Thanks to the photoconductive gain, optoelectronic printing can work at low optical intensities, even with an incoherent light source.[33, 74] This in turn reduces the cost of the laser required, providing a cost-effective means for on-demand fabrication of colloidal structures. The use of electric fields also offers additional possibilities to control the printing performance by tuning the AC/DC parameters. However, more studies are needed to fully understand the dependence of electrokinetic forces on the strength and frequency of the electric field, as well as the material and size of particles, to generalize this method for all kinds of colloidal particles.[70, 78] In addition, due to the diffraction limit of light the resolution of optoelectronic printing is relatively low, making single particle printing with nanoscale accuracy a challenge.

### Opto-Thermophoretic Printing.

Optothermal effects exploit entropically favorable photon-phonon conversion to generate heat,[38] which has been applied for various applications such as photothermal therapy,[79, 80] photothermal imaging,[81] and materials processing.[82] Recently, by harnessing the thermophoretic migration of colloidal species under an optical heating-created temperature gradient, opto-thermophoretic tweezers were developed to achieve low-power and versatile manipulation of colloidal particles, liposomes and biological cells.[83-86] Lin *et al.* reported reconfigurable opto-thermoelectric printing of colloidal particles *via* light-controlled thermoelectric fields.[87] A laser beam is focused on a plasmonic substrate composed of quasi-continuous AuNPs to create a well-defined temperature gradient by the plasmon-enhanced optothermal effect. Under the laser-generated thermal gradient, both $Na^+$ and $Cl^-$ ions migrate from the hot to the cold region (*i.e.*, move away from the laser spot) due to thermophoresis. The differences in the Soret coefficients (*i.e.*, $S_T$ ($Na^+$) > $S_T$ ($Cl^-$)) lead to the spatial separation of $Na^+$ and $Cl^-$ ions, establishing a thermoelectric field $E_T$ pointing from the cold to the hot region , which is given by:[41]

$$E_{\mathbf{T}} = \frac{k_B T \nabla T}{e} \frac{\sum_i Z_i n_i S_{Ti}}{\sum_i Z_i^2 n_i} \quad (2)$$

where $i$ indicates the ionic species ions ($Na^+$ and $Cl^-$), $k_B$ is the Boltzmann constant, $e$ is the elemental charge, $T$ is the environmental temperature, $\nabla T$ is the temperature gradient, and $Z_i$, $n_i$, and $S_{Ti}$ are the charge number, the concentration and the Soret coefficient of $i$ species, respectively.

Thus, Cetyltrimethylammonium chloride (CTAC)-functionalized polystyrene (PS) particles with positive charges were trapped at the laser spot by thermoelectric forces (Figure 5A). At a higher optical power, the depletion of CTAC micelles at the particle-substrate interfaces leads to the printing of particles *via* depletion attraction. Nanoparticles with variable sizes can be printed into arbitrary patterns with opto-thermoelectric printing (Figure 5B). By centering the laser beam back on the printed particle, CTAC micelles are driven into the particle-substrate gap, leading to release of the printed particle due to the repulsive electrostatic force between the CTAC micelles and the CTAC-coated particles overcoming depletion interactions. Reconfigurable printing was demonstrated by the selective release and reprinting one of the printed colloidal particles to realize the transformation of a “sad”-face pattern into a “smiley”-face pattern (Figure 5C).

CTAC micelles can also act as depletants to control the colloidal particle assembly by interparticle depletion attraction force. The incorporation of opto-thermoelectric fields with micelle-mediated depletion interactions enables the opto-thermophoretic assembly of colloidal matter into arbitrary configurations.[88] Peng *et al.* further demonstrated the opto-thermophoretic construction of colloidal superstructures in a photocurable hydrogel.[89] Particles were trapped and arranged into desired structures with thermoelectric fields and depletion attraction, and the assembled superstructures were then immobilized on substrates through UV cross-linking of the hydrogel (Figure 5D). Colloidal particles with various materials and sizes can be used as building blocks to construct diverse colloidal matter with controllable configurations and dimensions (Figure 5E). The as-built colloidal structures remained intact even after the samples were rinsed and dried, as confirmed by scanning electron microscopy (Figure 5E).

Opto-thermophoretic assembly and printing techniques provide a simple and reliable way to build colloidal superstructures with low optical power. The wide applicability of opto-thermophoretic techniques make them powerful tools to fabricate multifunctional colloidal nanomaterials and devices. Furthermore, the precise control of colloidal assembly configuration and the capacity for reconfigurable printing allow for tunable coupling between colloidal particles as well as the functions of the assemblies. Currently, generation of the thermal gradient relies on a quasi-continuous plasmonic substrate and a continuous-wave laser. The key to future development of opto-thermophoretic printing is the optimization of light-controlled temperature gradients. Specifically, further optimization of both the optothermally responsive substrate and the heating optics is highly desired. For instance, substrates with high photon-phonon conversion efficiencies and low thermal conductivities can be exploited to reduce the required optical power. Prepatterned substrates such as plasmonic nanoantenna arrays can serve as nanoheaters to manage the laser-induced hot spots with nanoscale precision.[90] Furthermore, using a pulsed laser as the heating source would further limit both heat transfer and collective heating on the substrates, optimizing the

temperature gradient and leading to a better general understanding of opto-thermophoretic printing.

### Opto-Thermomechanical Printing.

Opto-thermomechanical printing exploits the coupling between photothermal effects and mechanical forces to control the motion of nanoparticles. One strategy is called laser-induced transfer, which involves local melting of the donor film and ejection of small melted droplets towards the receiver substrate. This method has been applied for the fabrication of complex 2D and 3D microstructures consisting of plasmonic nanoparticles.[91, 92] Recently, Chichkov and coworkers reported optical printing of silicon nanoparticles with controlled optical properties based on such a laser-induced transfer strategy.[93] A tightly focused femtosecond laser is illuminated on a thin silicon film as the donor substrate, and absorption of light by the Si layer leads to ultrafast heating and local melting of this layer to form a droplet induced by surface tension. The generated droplet acquires an upward momentum during the droplet formation, driving it towards the receiver substrate (Figure 6A). The liquid material further solidifies at the receiver substrate surface to produce well-defined spherical nanoparticles. The diameter of Si nanoparticles can be varied by slightly increasing the laser pulse energy (Figure 6B). By irradiation with additional laser pulses, the laser-printed amorphous Si nanoparticles can be transformed into crystalline particles or into particles with mixed amorphous/crystalline phases. Laser-induced crystallization of Si nanoparticles results in a blue shift in the resonance peak and enhanced scattering efficiency (Figure 6C), providing a precise way to tune the optical properties of the fabricated particles. Besides Si, femtosecond laser printing of single crystalline Ge and SiGe nanoparticles was further demonstrated.[94] Such printed nanoparticles with controllable size and optical response are promising for nanophotonics and optoelectronics applications.

Another example of opto-thermomechanical approaches is to release nanoparticles from a donor substrate externally. For instance, Zhao and coworkers reported a release-and-place strategy to fabricate metallic nanostructures in air.[95] A laser is directed to AuNPs that are placed on a soft plastic donor substrate. The plasmon-enhanced heating of AuNPs leads to rapid surface expansion of the soft substrate, which results in the transfer of AuNPs to another receiver substrate (Figure 6D). Both in-plane and out-of-plane nanostructures can be fabricated in this way (Figure 6E). In comparison to laser-induced transfer, this method only requires a low-cost continuous-wave laser. In addition, the fabricated nanostructures are not limited to spherical shapes. Nanostructures with any desired shape can be nondestructively released from a donor substrate and additively transferred to another substrate. Further efforts are needed to improve the position control of the released nanoparticles. Potential strategies to enhance the fabrication accuracy include improving the flatness of the donor substrate, optimizing the separation distance between the receiver and the donor substrate, and applying an external field to guide the motion of particles.

Laser-induced transfer provides a simple and single-step approach to simultaneously fabricate and pattern colloidal particles with tailorable sizes. However, opto-thermomechanical methods rely on the photothermal effects of the donor film or the targeted

particle. Thus, an inherent limitation to this technique is that it is only applicable to materials with an optothermal response.

### Bubble Printing.

Microbubbles can be generated by laser heating of metal nanostructures due to plasmon-enhanced optothermal effects.[96, 97] Optothermal bubbles have enabled many intriguing applications including plasmofluidic lenses,[98] particle trapping,[99] photothermal motors,[100] and cell manipulation.[101] Recently, Zheng and coworkers developed bubble-pen lithography (BPL) to achieve patterning of colloidal particles by optically controlled microbubbles (Figure 7A).[102] A focused laser beam is directed onto a plasmonic substrate, and the resulting plasmon-enhanced heating creates a microbubble at the interface between the substrate and the colloidal suspension due to water vaporization. Convective flow caused by the temperature gradient drags the colloidal particles down to the plasmonic substrate. Particles are then driven toward the microbubble *via* Marangoni convection induced by the stress tension gradient at the bubble surface (Figure 7B) and immobilized on the substrate by van der Waals interactions. The microbubble diameter and the size of the printed colloidal assemblies can be precisely controlled by tuning the optical power density (Figure 7C). BPL can also be used to print particles with a wide range of sizes (Figure 7D), which is desired for printing multiscale structures. By steering the laser beam and controlling the on/off state of the laser, BPL can realize both continuous writing of particle assemblies and one-by-one patterning of single particles into arbitrary patterns.

BPL was applied for programmable and high-throughput patterning of semiconductor QDs.[103] Large-area uniform patterns composed of QDs were created by scanning the laser beam (Figure 7E). Figure 7F shows a U.S. map where the states of Texas, California, and Pennsylvania are printed with different QDs fabricated by a multistep printing process, demonstrating the potential for full-color QD printing. Pattering QDs on flexible substrates was also achieved and the printed QDs can withstand the bending of the substrates, which shows promise for future use in flexible devices. Rajeeva *et al.* further integrated BPL with a smartphone to develop a haptic interface for facile control of bubble printing (Figure 7G).[104] This haptic interface enables free-form patterning of QDs by simply controlling hand movement over the smartphone display.

Besides colloidal particles, BPL also demonstrated the capability for single-step site-specific fabrication of metallic nanostructures.[105] Large-scale uniform Ag rings are fabricated from a Ag precursor using an optically-controlled microbubble (Figure 7H), where Ag ring size can be controlled by laser power. The tunable Ag ring arrays exhibit surface plasmon resonances in the mid-infrared regime from 3.8 to 4.6 μm (Figure 7I) and showed excellent performance as a surface-enhanced infrared spectroscopy substrate.

Compared with other optical printing techniques, BPL has shown versatility in direct printing of low-dimensional objects of diverse sizes (several nanometers to microscale) and materials (dielectric, semiconductor and metallic). However, high temperature from plasmonic heating is required to generate optothermal bubbles, and such heat and related cavitation effects resulting from plasmonic heating[106] can cause damage to fragile biological objects such as cells. Additionally, the printing of nanoscale colloids at single-particle

resolution is still challenging. This can be potentially addressed through engineering of the substrate, such as patterning with isolated plasmonic nanoantennas, to generate nanosized bubbles.

### Photochemical Printing.

Photochemical reactions provide a facile strategy for light-directed synthesis and functionalization of various nanoparticles with well-controlled sizes, shapes, and properties.[107-111] Photochemistry has been extensively applied to control the coordination of nanoparticles with other nanoparticles and surfaces through the photochemical formation and breakage of covalent bonds. Therefore, photochemical printing of colloidal particles can be achieved by applying light-controlled chemical reactions to anchor or immobilize surface-functionalized nanoparticles.[112-115]

Many different strategies toward photochemical printing of colloidal particles have been developed in the last decade. For instance, immobilization of $TiO_2$ nanorods and $\gamma$-$Fe_2O_3$ nanocrystals passivated with unsaturated long-chain carboxylic acids on hydrogenated silicon was realized by a UV-induced hydrosilylation reaction.[116] Similarly, the anchoring of surfactant-modified AuNPs and magnetic nanoparticles on hydrogen-terminated silicon by UV irradiation was also demonstrated.[117, 118] Recently, Fischer and coworkers reported *in situ* immobilization of dynamic assemblies of colloidal particles by UV-triggered click-chemistry.[43] The underlying click reaction is the “thiol-yne” alkyne hydrothiolation, which is an organic reaction between a thiol and an alkyne to form a covalent bond (Figure 8A). This reaction is fast, efficient, general to arbitrary particles, and can work in the presence of external optical and magnetic fields. Functionalized particles can be permanently captured onto functionalized glass surface with just a few seconds of UV irradiation. In combination with optical tweezers used to trap particles at desired locations and in arbitrary configurations, this photoclick strategy can be applied for fast and dynamic fabrication of colloidal microstructures (Figure 8B). However, the surface functionalization of particles may increase experimental complexity and lead to undesired effects in practical applications.[119]

## PERSPECTIVE

The gamut of state-of-the-art approaches discussed herein show that a broad set of physical mechanisms can be harnessed for optical nano-printing of colloidal particles with various compositions and sizes. Despite of the numerous achievements in recent years, grand challenges and opportunities remain in improving the strengths of optical nano-printing in terms of printing precision, throughput, 3D printing, materials applicability, multiscale printing, and functionalities (Figure 9).

Optical nano-printing using colloidal particles as building blocks has the advantage of single particle-level resolution. Thus, it provides an effective strategy for fabrication of colloidal nanostructures for optical coupling investigation and photonic nanodevices.[120, 121] However, the precise control of printing position at nanoscale is still challenging due to the diffraction limit, which may impair the capability of optical printing. Considering the multitude of strategies developed in the semiconductor industry for increasing the resolution of

photolithographic processes (deep UV, high refractive index media, interference patterns), there may be similar approaches that are applicable for such optical printing techniques. The accuracy and resolution can be potentially improved by substrate engineering and near-field optics. For instance, plasmonic nanoantennas with strong near-field enhancement are able to trap particle to targeted position with nanometer resolution.[122] For the scalable manufacturing of colloidal nanostructures, one should also improve the throughput of current optical printing techniques. The use of a digital micromirror device or a spatial light modulator to multiply working laser beam allows parallel printing of particles.[53, 87] An alternative promising direction for the improvement of throughput is to exploit well-developed microfluidics for continuous and automated operation.

So far, optical nano-printing has proved powerful for the construction of 2D nanostructures. Although construction of 3D assemblies was demonstrated,[89, 95] the number of particles in the 3D nanostructures and their configuration are still limited. This limitation can be potentially addressed by using optical fibers to achieve 3D printing *via* control over the focus along the z-axis. Another future direction is to study the wide applicability of optical printing for various materials (*e.g.*, plasmonic, dielectric, polymer, and semiconductor) at different scales (from microparticles to quantum dots). For instance, thorough understanding and rational optimization of drift characteristics (*e.g.*, thermophoresis, dielectrophoresis, and thermo-capillary flows), as well as surface chemistry of the colloidal particles, will provide insights and guidelines to help enhance the capabilities for a number of optical printing techniques.

Last but not least, one should explore the versatility of optical nano-printing in fabrication of colloidal nanostructures for functional micro-/nano-devices. For example, optically patterned AuNP arrays can fully function as micro-diffraction gratings.[53] Gold microwires fabricated by direct laser writing of gold nanodots can be applied for electric connection of electronic microdevices.[61] Furthermore, the ability to print various quantum dots demonstrates the potential of optical printing techniques for fabricating full-color displays.[103] The capability to create multi-component colloidal superstructures will further enable a variety of lab-on-chip devices such as reconfigurable metamaterials, photonic crystals, colloidal waveguides, and sensors. Precise printing at single particle resolution also provide the opportunities for a wide range of applications. For instance, optical printing of a seed nanoparticle provides a powerful tool to study chemical reactions at the single particle level.[123] Accurate positioning of a single nanoparticle onto a photonic crystal nanocavity provides a powerful tool for the design of functional photonic devices and sensors.[124]

## SUMMARY

Over the past few years, significant developments have led to the use of lasers to print a wide variety of materials down to nanoscale dimensions *via* diverse physical mechanisms. With its capability to build arbitrary nanostructures at single-particle resolution, optical nano-printing holds great potential as a nanofabrication tool to surpass conventional techniques. Due to its significance in both scientific research and modern nanotechnology, optical nano-printing will be widely explored in the future. As this field continues to develop, we believe

the versatile capabilities of optical nano-printing will facilitate exciting advances in microelectronics, nanophotonics, colloidal sciences, biology and beyond.

## ACKNOWLEDGEMENTS

J.L., L.L. and Y.Z. acknowledges the financial supports of the Beckman Young Investigator Program, the Army Research Office (W911NF-17-1-0561), the National Aeronautics and Space Administration Early Career Faculty Award (80NSSC17K0520), the National Science Foundation (NSF-CMMI-1761743) and the National Institute of General Medical Sciences of the National Institutes of Health (DP2GM128446). E.H.H. acknowledges support by the German Academic Exchange Service (DAAD), from funds of the German Federal Ministry of Education and Research (BMBF) (57429511).

## VOCABULARY

**optical nano-printing**
the process of using a laser to control the construction of micro-/nano-structures

**colloidal particles**
microscopic solid particles that are suspended in a fluid phase with a typical size range between ~10 nm and several microns

**optical forces**
the forces exerted on colloidal particles directly by a laser beam

**optoelectric field**
a light-controlled electric field in photosensitive systems

**optothermal effect**
the conversion of optical energy into thermal energy through photon-phonon conversion

**photochemical reaction**
a chemical reaction that is controlled by light

## REFERENCES

(1). Vieu C; Carcenac F; Pepin A; Chen Y; Mejias M; Lebib A; Manin-Ferlazzo L; Couraud L; Launois H Electron Beam Lithography: Resolution Limits and Applications. Appl. Surf. Sci 2000, 164, 111–117.

(2). Ye X; Jin L; Caglayan H; Chen J; Xing G; Zheng C; Doan-Nguyen V; Kang Y; Engheta N; Kagan CR; Murray CB Improved Size-Tunable Synthesis of Monodisperse Gold Nanorods through the Use of Aromatic Additives. ACS Nano 2012, 6, 2804–2817. [PubMed: 22376005]

(3). Gonzalez-Rubio G; Guerrero-Martinez A; Liz-Marzan LM Reshaping, Fragmentation, and Assembly of Gold Nanoparticles Assisted by Pulse Lasers. Acc. Chem. Res 2016, 49, 678–686. [PubMed: 27035211]

(4). Matijevic E Production of Monodispersed Colloidal Particles. Ann. Rev. Mater. Sci 1985, 15, 483–516.

(5). Yang S-M; Kim S-H; Lim J-M; Yi G-R Synthesis and Assembly of Structured Colloidal Particles. J. Mater. Chem 2008, 18, 2177–2190.

(6). Talapin DV; Lee JS; Kovalenko MV; Shevchenko EV Prospects of Colloidal Nanocrystals for Electronic and Optoelectronic Applications. Chem. Rev 2010, 110, 389–458. [PubMed: 19958036]

(7). Kim JW; Larsen RJ; Weitz DA Synthesis of Nonspherical Colloidal Particles with Anisotropic Properties. J. Am. Chem. Soc 2006, 128, 14374–14377. [PubMed: 17076511]

(8). Xia Y; Halas NJ Shape-Controlled Synthesis and Surface Plasmonic Properties of Metallic Nanostructures. MRS Bull. 2005, 30, 338–348.

(9). Whitesides GM; Grzybowski B Self-Assembly at All Scales. Science 2002, 295, 2418–2421. [PubMed: 11923529]

(10). Zhang M; Magagnosc DJ; Liberal I; Yu Y; Yun H; Yang H; Wu Y; Guo J; Chen W; Shin YJ; Stein A; Kikkawa JM; Engheta N; Gianola DS; Murray CB; Kagan CR High-Strength Magnetically Switchable Plasmonic Nanorods Assembled from a Binary Nanocrystal Mixture. Nat. Nanotechnol 2016, 12, 228. [PubMed: 27819691]

(11). Greybush NJ; Saboktakin M; Ye X; Della Giovampaola C; Oh SJ; Berry NE; Engheta N; Murray CB; Kagan CR Plasmon-Enhanced Upconversion Luminescence in Single Nanophosphor–Nanorod Heterodimers Formed through Template-Assisted Self-Assembly. ACS Nano 2014, 8, 9482–9491. [PubMed: 25182662]

(12). Greybush NJ; Pacheco-Pena V; Engheta N; Murray CB; Kagan CR Plasmonic Optical and Chiroptical Response of Self-Assembled Au Nanorod Equilateral Trimers. ACS Nano 2019, 13, 1617–1624. [PubMed: 30629426]

(13). Hanske C; Hill EH; Vila-Liarte D; González-Rubio G; Matricardi C; Mihi A; Liz-Marzán LM Solvent-Assisted Self-Assembly of Gold Nanorods into Hierarchically Organized Plasmonic Mesostructures. ACS Appl. Mater. Interfaces 2019, DOI: 10.1021/acsami.9b00334.

(14). Urban AS; Lutich AA; Stefani FD; Feldmann J Laser Printing Single Gold Nanoparticles. Nano Lett 2010, 10, 4794–4798. [PubMed: 20957994]

(15). Stohr RJ; Kolesov R; Xia K; Wrachtrup J All-Optical High-Resolution Nanopatterning and 3D Suspending of Graphene. ACS Nano 2011, 5, 5141–5150. [PubMed: 21595474]

(16). Lin L; Hill EH; Peng X; Zheng Y Optothermal Manipulations of Colloidal Particles and Living Cells. Acc. Chem. Res 2018, 51, 1465–1474. [PubMed: 29799720]

(17). Urbach JC; Fisli TS; Starkweather GK Laser Scanning for Electronic Printing. Proc. IEEE 1982, 70, 597–618.

(18). Shen X; Asenjo-Garcia A; Liu Q; Jiang Q; Garcia de Abajo FJ; Liu N; Ding B Three-Dimensional Plasmonic Chiral Tetramers Assembled by DNA Origami. Nano Lett 2013, 13, 2128–2133. [PubMed: 23600476]

(19). Cecconello A; Besteiro LV; Govorov AO; Willner I Chiroplasmonic DNA-Based Nanostructures. Nat. Rev. Mater 2017, 2, 17039.

(20). Maier SA; Brongersma ML; Kik PG; Meltzer S; Requicha AAG; Atwater HA Plasmonics—a Route to Nanoscale Optical Devices. Adv. Mater 2001, 13, 1501–1505.

(21). Shi J; Monticone F; Elias S; Wu Y; Ratchford D; Li X; Alu A Modular Assembly of Optical Nanocircuits. Nat. Commun 2014, 5, 3896. [PubMed: 24871450]

(22). Li M; Lohmüller T; Feldmann J Optical Injection of Gold Nanoparticles into Living Cells. Nano Lett 2015, 15, 770–775. [PubMed: 25496343]

(23). Urban AS; Pfeiffer T; Fedoruk M; Lutich AA; Feldmann J Single-Step Injection of Gold Nanoparticles through Phospholipid Membranes. ACS Nano 2011, 5, 3585–3590. [PubMed: 21488672]

(24). Mio C; Marr DWM Optical Trapping for the Manipulation of Colloidal Particles. Adv. Mater 2000, 12, 917–920.

(25). Shaw LA; Chizari S; Panas RM; Shusteff M; Spadaccini CM; Hopkins JB Holographic Optical Assembly and Photopolymerized Joining of Planar Microspheres. Opt. Lett 2016, 41, 3571–3574. [PubMed: 27472621]

(26). Burns MM; Fournier J-M; Golovchenko JA Optical Binding. Phys. Rev. Lett 1989, 63, 1233–1236. [PubMed: 10040510]

(27). Mohanty SK; Andrews JT; Gupta PK Optical Binding Between Dielectric Particles. Opt. Express 2004, 12, 2746–2753. [PubMed: 19475117]

(28). Bao Y; Yan Z; Scherer NF Optical Printing of Electrodynamically Coupled Metallic Nanoparticle Arrays. J. Phys. Chem. C 2014, 118, 19315–19321.

(29). Jonas A; Zemanek P Light at Work: The Use of Optical Forces for Particle Manipulation, Sorting, and Analysis. Electrophoresis 2008, 29, 4813–4851. [PubMed: 19130566]

(30). Swartzlander GA Jr; Peterson TJ; Artusio-Glimpse AB; Raisanen AD Stable Optical Lift. Nat. Photonics 2010, 5, 48–51.

(31). Xu H; Kall M Surface-Plasmon-Enhanced Optical Forces in Silver Nanoaggregates. Phys. Rev. Lett 2002, 89, 246802. [PubMed: 12484969]

(32). Chiou PY; Ohta AT; Wu MC Massively Parallel Manipulation of Single Cells and Microparticles Using Optical Images. Nature 2005, 436, 370–372. [PubMed: 16034413]

(33). Wu MC Optoelectronic Tweezers. Nat. Photonics 2011, 5, 322.

(34). Williams SJ; Kumar A; Green NG; Wereley ST A Simple, Optically Induced Electrokinetic Method to Concentrate and Pattern Nanoparticles. Nanoscale 2009, 1, 133–137. [PubMed: 20644872]

(35). Huang K-W; Wu Y-C; Lee J-A; Chiou P-Y Microfluidic Integrated Optoelectronic Tweezers for Single-Cell Preparation and Analysis. Lab Chip 2013, 13, 3721–3727. [PubMed: 23884358]

(36). Huang K-W; Su T-W; Ozcan A; Chiou P-Y Optoelectronic Tweezers Integrated with Lensfree Holographic Microscopy for Wide-Field Interactive Cell and Particle Manipulation on a Chip. Lab Chip 2013, 13, 2278–2284. [PubMed: 23661233]

(37). Li J; Lin L; Inoue Y; Zheng Y Opto-Thermophoretic Tweezers and Assembly. J. Micro Nano-Manuf 2018, 6, 040801.

(38). Baffou G; Quidant R Thermo-Plasmonics: Using Metallic Nanostructures as Nano-Sources of Heat. Laser Photonics Rev 2013, 7, 171–187.

(39). Roberto P 'Thermal Forces': Colloids in Temperature Gradients. J. Phys.: Condens. Matter 2004, 16, S4195.

(40). Alois W Thermal Non-Equilibrium Transport in Colloids. Rep. Prog. Phys 2010, 73, 126601.

(41). Reichl M; Herzog M; Gotz A; Braun D Why Charged Molecules Move Across a Temperature Gradient: The Role of Electric Fields. Phys. Rev. Lett 2014, 112, 198101. [PubMed: 24877967]

(42). Xu X; Luo J Marangoni Flow in an Evaporating Water Droplet. Appl. Phys. Lett 2007, 91, 124102.

(43). Walker D; Singh DP; Fischer P Capture of 2D Microparticle Arrays *via* a UV-Triggered Thiol-Yne "Click" Reaction. Adv. Mater 2016, 28, 9846–9850. [PubMed: 27717081]

(44). Ashkin A; Dziedzic JM; Bjorkholm JE; Chu S Observation of a Single-Beam Gradient Force Optical Trap for Dielectric Particles. Opt. Lett 1986, 11, 288. [PubMed: 19730608]

(45). Ashkin A; Dziedzic JM Optical Trapping and Manipulation of Viruses and Bacteria. Science 1987, 235, 1517–1520. [PubMed: 3547653]

(46). Ashkin A; Dziedzic JM; Yamane T Optical Trapping and Manipulation of Single Cells Using Infrared Laser Beams. Nature 1987, 330, 769–771. [PubMed: 3320757]

(47). Ashkin A Optical Trapping and Manipulation of Neutral Particles Using Lasers. Proc. Natl. Acad. Sci. U. S. A 1997, 94, 4853–4860. [PubMed: 9144154]

(48). Grier DG A Revolution in Optical Manipulation. Nature 2003, 424, 810–816. [PubMed: 12917694]

(49). Hoogenboom JP; Vossen DLJ; Faivre-Moskalenko C; Dogterom M; Blaaderen A. v. Patterning Surfaces with Colloidal Particles Using Optical Tweezers. Appl. Phys. Lett 2002, 80, 4828–4830.

(50). Ito S; Yoshikawa H; Masuhara H Laser Manipulation and Fixation of Single Gold Nanoparticles in Solution at Room Temperature. Appl. Phys. Lett 2002, 80, 482–484.

(51). Ling L; Guo H-L; Zhong X-L; Huang L; Li J-F; Gan L; Li Z-Y Manipulation of Gold Nanorods with Dual-Optical Tweezers for Surface Plasmon Resonance Control. Nanotechnology 2012, 23, 215302. [PubMed: 22551556]

(52). Guffey MJ; Scherer NF All-Optical Patterning of Au Nanoparticles on Surfaces Using Optical Traps. Nano Lett 2010, 10, 4302–4308. [PubMed: 20925400]

(53). Nedev S; Urban AS; Lutich AA; Feldmann J Optical Force Stamping Lithography. Nano Lett 2011, 11, 5066–5070. [PubMed: 21992538]

(54). Guffey MJ; Miller RL; Gray SK; Scherer NF Plasmon-Driven Selective Deposition of Au Bipyramidal Nanoparticles. Nano Lett 2011, 11, 4058–4066. [PubMed: 21902194]

(55). Do J; Fedoruk M; Jackel F; Feldmann J Two-Color Laser Printing of Individual Gold Nanorods. Nano Lett 2013, 13, 4164–4168. [PubMed: 23927535]

(56). Urban AS; Fedoruk M; Nedev S; Lutich A; Lohmueller T; Feldmann J Shrink-to-Fit Plasmonic Nanostructures. Adv. Opt. Mater 2013, 1, 123–127.

(57). Gargiulo J; Cerrota S; Cortes E; Violi IL; Stefani FD Connecting Metallic Nanoparticles by Optical Printing. Nano Lett 2016, 16, 1224–1229. [PubMed: 26745330]

(58). Gargiulo J; Brick T; Violi IL; Herrera FC; Shibanuma T; Albella P; Requejo FG; Cortes E; Maier SA; Stefani FD Understanding and Reducing Photothermal Forces for the Fabrication of Au Nanoparticle Dimers by Optical Printing. Nano Lett 2017, 17, 5747–5755. [PubMed: 28806511]

(59). Wang K; Schonbrun E; Steinvurzel P; Crozier KB Trapping and Rotating Nanoparticles Using a Plasmonic Nano-Tweezer with an Integrated Heat Sink. Nat. Commun 2011, 2, 469. [PubMed: 21915111]

(60). Balandin AA; Ghosh S; Bao W; Calizo I; Teweldebrhan D; Miao F; Lau CN Superior Thermal Conductivity of Single-Layer Graphene. Nano Lett 2008, 8, 902–907. [PubMed: 18284217]

(61). Xu BB; Zhang R; Wang H; Liu XQ; Wang L; Ma ZC; Chen QD; Xiao XZ; Han B; Sun HB Laser Patterning of Conductive Gold Micronanostructures from Nanodots. Nanoscale 2012, 4, 6955–6958. [PubMed: 23044631]

(62). Wang H; Liu S; Zhang YL; Wang JN; Wang L; Xia H; Chen QD; Ding H; Sun HB Controllable Assembly of Silver Nanoparticles Induced by Femtosecond Laser Direct Writing. Sci. Technol. Adv. Mater 2015, 16, 024805. [PubMed: 27877766]

(63). Xu B-B; Zhang Y-L; Zhang R; Wang L; Xiao X-Z; Xia H; Chen Q-D; Sun H-B Programmable Assembly of CdTe Quantum Dots into Microstructures by Femtosecond Laser Direct Writing. J. Mater. Chem. C 2013, 1, 4699–4704.

(64). Wang H; Zhang Y-L; Xia H; Chen Q-D; Lee K-S; Sun H-B Photodynamic Assembly of Nanoparticles Towards Designable Patterning. Nanoscale Horiz 2016, 1, 201–211.

(65). Ma Z-C; Zhang Y-L; Han B; Chen Q-D; Sun H-B Femtosecond-Laser Direct Writing of Metallic Micro/Nanostructures: From Fabrication Strategies to Future Applications. Small Methods 2018, 2, 1700413.

(66). Zaza C; Violi IL; Gargiulo J; Chiarelli G; Langolf L; Jakobi J; Olmos J; Cortes E; Koenig M; Barcikowski S; Schlücker S; Saenz JJ; Maier SA; Stefani FD Size-Selective Optical Printing of Silicon Nanoparticles through Their Dipolar Magnetic Resonance. ACS Photonics 2019, DOI: 10.1021/acsphotonics.8b01619.

(67). Babynina A; Fedoruk M; Kühler P; Meledin A; Döblinger M; Lohmüller T Bending Gold Nanorods with Light. Nano Lett 2016, 16, 6485–6490. [PubMed: 27598653]

(68). Pethig R Review Article—Dielectrophoresis: Status of the Theory, Technology, and Applications. Biomicrofluidics 2010, 4, 022811. [PubMed: 20697589]

(69). Williams SJ; Kumar A; Wereley ST Electrokinetic Patterning of Colloidal Particles with Optical Landscapes. Lab Chip 2008, 8, 1879–1882. [PubMed: 18941688]

(70). Kumar A; Kwon JS; Williams SJ; Green NG; Yip NK; Wereley ST Optically Modulated Electrokinetic Manipulation and Concentration of Colloidal Particles near an Electrode Surface. Langmuir 2010, 26, 5262–5272. [PubMed: 20232836]

(71). Gascoyne PRC; Vykoukal J Particle Separation by Dielectrophoresis. 2002, 23, 1973–1983.

(72). Hölzel R; Calander N; Chiragwandi Z; Willander M; Bier FF Trapping Single Molecules by Dielectrophoresis. Phys. Rev. Lett 2005, 95, 128102. [PubMed: 16197115]

(73). Nadappuram BP; Cadinu P; Barik A; Ainscough AJ; Devine MJ; Kang M; Gonzalez-Garcia J; Kittler JT; Willison KR; Vilar R; Actis P; Wojciak-Stothard B; Oh S-H; Ivanov AP; Edel JB Nanoscale Tweezers for Single-Cell Biopsies. Nat. Nanotechnol 2019, 14, 80–88. [PubMed: 30510280]

(74). Jamshidi A; Neale SL; Yu K; Pauzauskie PJ; Schuck PJ; Valley JK; Hsu HY; Ohta AT; Wu MC Nanopen: Dynamic, Low-Power, and Light-Actuated Patterning of Nanoparticles. Nano Lett 2009, 9, 2921–2925. [PubMed: 19588985]

(75). Hayward RC; Saville DA; Aksay IA Electrophoretic Assembly of Colloidal Crystals with Optically Tunable Micropatterns. Nature 2000, 404, 56–59. [PubMed: 10716438]

(76). Pascall AJ; Qian F; Wang G; Worsley MA; Li Y; Kuntz JD Light-Directed Electrophoretic Deposition: A New Additive Manufacturing Technique for Arbitrarily Patterned 3D Composites. Adv. Mater 2014, 26, 2252–2256. [PubMed: 24532281]

(77). Rodrigo JA Fast Optoelectric Printing of Plasmonic Nanoparticles into Tailored Circuits. Sci. Rep 2017, 7, 46506. [PubMed: 28406226]

(78). Ng WY; Goh S; Lam YC; Yang C; Rodriguez I DC-Biased AC-Electroosmotic and AC-Electrothermal Flow Mixing in Microchannels. Lab Chip 2009, 9, 802–809. [PubMed: 19255662]

(79). Huang X; El-Sayed IH; Qian W; El-Sayed MA Cancer Cell Imaging and Photothermal Therapy in the near-Infrared Region by Using Gold Nanorods. J. Am. Chem. Soc 2006, 128, 2115–2120. [PubMed: 16464114]

(80). El-Sayed IH; Huang X; El-Sayed MA Selective Laser Photo-Thermal Therapy of Epithelial Carcinoma Using Anti-Egfr Antibody Conjugated Gold Nanoparticles. Cancer Lett 2006, 239, 129–135. [PubMed: 16198049]

(81). Boyer D; Tamarat P; Maali A; Lounis B; Orrit M Photothermal Imaging of Nanometer-Sized Metal Particles among Scatterers. Science 2002, 297, 1160–1163. [PubMed: 12183624]

(82). Lin L; Li J; Li W; Yogeesh MN; Shi J; Peng X; Liu Y; Rajeeva BB; Becker MF; Liu Y; Akinwande D; Zheng Y Optothermoplasmonic Nanolithography for on-Demand Patterning of 2D Materials. Adv. Funct. Mater 2018, 28, 1803990.

(83). Lin L; Peng X; Wei X; Mao Z; Xie C; Zheng Y Thermophoretic Tweezers for Low-Power and Versatile Manipulation of Biological Cells. ACS Nano 2017, 11, 3147–3154. [PubMed: 28230355]

(84). Lin L; Wang M; Peng X; Lissek EN; Mao Z; Scarabelli L; Adkins E; Coskun S; Unalan HE; Korgel BA; Liz-Marzan LM; Florin EL; Zheng Y Opto-Thermoelectric Nanotweezers. Nat. Photonics 2018, 12, 195–201. [PubMed: 29785202]

(85). Lin L; Peng X; Mao Z; Wei X; Xie C; Zheng Y Interfacial-Entropy-Driven Thermophoretic Tweezers. Lab Chip 2017, 17, 3061–3070. [PubMed: 28805878]

(86). Hill EH; Li J; Lin L; Liu Y; Zheng Y Opto-Thermophoretic Attraction, Trapping, and Dynamic Manipulation of Lipid Vesicles. Langmuir 2018, 34, 13252–13262. [PubMed: 30350700]

(87). Lin L; Peng X; Zheng Y Reconfigurable Opto-Thermoelectric Printing of Colloidal Particles. Chem. Commun 2017, 53, 7357–7360.

(88). Lin L; Zhang J; Peng X; Wu Z; Coughlan ACH; Mao Z; Bevan MA; Zheng Y Opto-Thermophoretic Assembly of Colloidal Matter. Sci. Adv 2017, 3, e1700458. [PubMed: 28913423]

(89). Peng X; Li J; Lin L; Liu Y; Zheng Y Opto-Thermophoretic Manipulation and Construction of Colloidal Superstructures in Photocurable Hydrogels. ACS Appl. Nano Mater 2018, 1, 3998–4004.

(90). Liu Y; Lin L; Bangalore Rajeeva B; Jarrett JW; Li X; Peng X; Kollipara P; Yao K; Akinwande D; Dunn AK; Zheng Y Nanoradiator-Mediated Deterministic Opto-Thermoelectric Manipulation. ACS Nano 2018, 12, 10383–10392. [PubMed: 30226980]

(91). Kuznetsov AI; Koch J; Chichkov BN Laser-Induced Backward Transfer of Gold Nanodroplets. Opt. Express 2009, 17, 18820–18825. [PubMed: 20372615]

(92). Kuznetsov AI; Kiyan R; Chichkov BN Laser Fabrication of 2D and 3D Metal Nanoparticle Structures and Arrays. Opt. Express 2010, 18, 21198–21203. [PubMed: 20941016]

(93). Zywietz U; Evlyukhin AB; Reinhardt C; Chichkov BN Laser Printing of Silicon Nanoparticles with Resonant Optical Electric and Magnetic Responses. Nat. Commun 2014, 5, 3402. [PubMed: 24595073]

(94). Zhigunov DM; Evlyukhin AB; Shalin AS; Zywietz U; Chichkov BN Femtosecond Laser Printing of Single Ge and SiGe Nanoparticles with Electric and Magnetic Optical Resonances. ACS Photonics 2018, 5, 977–983.

(95). Alam MS; Zhao C Nondestructive Approach for Additive Nanomanufacturing of Metallic Nanostructures in the Air. ACS Omega 2018, 3, 1213–1219.

(96). Fang Z; Zhen YR; Neumann O; Polman A; Garcia de Abajo FJ; Nordlander P; Halas NJ Evolution of Light-Induced Vapor Generation at a Liquid-Immersed Metallic Nanoparticle. Nano Lett 2013, 13, 1736–1742. [PubMed: 23517407]

(97). Baffou G; Polleux J; Rigneault H; Monneret S Super-Heating and Micro-Bubble Generation around Plasmonic Nanoparticles under CW Illumination. J. Phys. Chem. C 2014, 118, 4890–4898.

(98). Zhao C; Liu Y; Zhao Y; Fang N; Huang TJ A Reconfigurable Plasmofluidic Lens. Nat. Commun 2013, 4, 2305. [PubMed: 23929463]

(99). Zhao C; Xie Y; Mao Z; Zhao Y; Rufo J; Yang S; Guo F; Mai JD; Huang TJ Theory and Experiment on Particle Trapping and Manipulation *via* Optothermally Generated Bubbles. Lab Chip 2014, 14, 384–391. [PubMed: 24276624]

(100). Meng F; Hao W; Yu S; Feng R; Liu Y; Yu F; Tao P; Shang W; Wu J; Song C; Deng T Vapor-Enabled Propulsion for Plasmonic Photothermal Motor at the Liquid/Air Interface. J. Am. Chem. Soc 2017, 139, 12362–12365. [PubMed: 28837327]

(101). Karim F; Vasquez ES; Zhao C Fabricated Nanogap-Rich Plasmonic Nanostructures through an Optothermal Surface Bubble in a Droplet. Opt. Lett 2018, 43, 334–336. [PubMed: 29328275]

(102). Lin L; Peng X; Mao Z; Li W; Yogeesh MN; Rajeeva BB; Perillo EP; Dunn AK; Akinwande D; Zheng Y Bubble-Pen Lithography. Nano Lett 2016, 16, 701–708. [PubMed: 26678845]

(103). Bangalore Rajeeva B; Lin L; Perillo EP; Peng X; Yu WW; Dunn AK; Zheng Y High-Resolution Bubble Printing of Quantum Dots. ACS Appl. Mater, Interfaces 2017, 9, 16725–16733. [PubMed: 28452214]

(104). Rajeeva BB; Alabandi MA; Lin L; Perillo EP; Dunn AK; Zheng Y Patterning and Fluorescence Tuning of Quantum Dots with Haptic-Interfaced Bubble Printing. J. Mater. Chem. C 2017, 5, 5693–5699.

(105). Rajeeva BB; Wu Z; Briggs A; Acharya PV; Walker SB; Peng X; Bahadur V; Bank SR; Zheng Y "Point-and-Shoot" Synthesis of Metallic Ring Arrays and Surface-Enhanced Optical Spectroscopy. Adv. Opt. Mater 2018, 6, 1701213.

(106). Boulais É; Lachaine R; Meunier M Plasma-Mediated Nanocavitation and Photothermal Effects in Ultrafast Laser Irradiation of Gold Nanorods in Water. J. Phys. Chem. C 2013, 117, 9386–9396.

(107). Pietrobon B; Kitaev V Photochemical Synthesis of Monodisperse Size-Controlled Silver Decahedral Nanoparticles and Their Remarkable Optical Properties. Chem. Mater 2008, 20, 5186–5190.

(108). Kim F; Song JH; Yang P Photochemical Synthesis of Gold Nanorods. J. Am. Chem. Soc 2002, 124, 14316–14317. [PubMed: 12452700]

(109). Maretti L; Billone PS; Liu Y; Scaiano JC Facile Photochemical Synthesis and Characterization of Highly Fluorescent Silver Nanoparticles. J. Am. Chem. Soc 2009, 131, 13972–13980. [PubMed: 19788331]

(110). McGilvray KL; Decan MR; Wang D; Scaiano JC Facile Photochemical Synthesis of Unprotected Aqueous Gold Nanoparticles. J. Am. Chem. Soc 2006, 128, 15980–15981. [PubMed: 17165719]

(111). Yang XY; Sun M; Bian YX; He XM A Room-Temperature High-Conductivity Metal Printing Paradigm with Visible-Light Projection Lithography. Adv. Funct. Mater 2019, 29.

(112). Huang X; Zhou X; Wu S; Wei Y; Qi X; Zhang J; Boey F; Zhang H Reduced Graphene Oxide-Templated Photochemical Synthesis and *in situ* Assembly of Au Nanodots to Orderly Patterned Au Nanodot Chains. Small 2010, 6, 513–516. [PubMed: 20077425]

(113). Xu B-B; Wang L; Ma Z-C; Zhang R; Chen Q-D; Lv C; Han B; Xiao X-Z; Zhang X-L; Zhang Y-L; Ueno K; Misawa H; Sun H-B Surface-Plasmon-Mediated Programmable Optical Nanofabrication of an Oriented Silver Nanoplate. ACS Nano 2014, 8, 6682–6692. [PubMed: 24896225]

(114). McGilvray KL; Fasciani C; Bueno-Alejo CJ; Schwartz-Narbonne R; Scaiano JC Photochemical Strategies for the Seed-Mediated Growth of Gold and Gold–Silver Nanoparticles. Langmuir 2012, 28, 16148–16155. [PubMed: 23130742]

(115). Zhang Y; Zhang Q; Ouyang X; Lei DY; Zhang AP; Tam H-Y Ultrafast Light-Controlled Growth of Silver Nanoparticles for Direct Plasmonic Color Printing. ACS Nano 2018, 12, 9913–9921. [PubMed: 30153416]

(116). Fanizza E; Cozzoli PD; Curri ML; Striccoli M; Sardella E; Agostiano A UV-Light-Driven Immobilization of Surface-Functionalized Oxide Nanocrystals onto Silicon. Adv. Funct. Mater 2007, 17, 201–211.

(117). Leem G; Zhang S; Jamison AC; Galstyan E; Rusakova I; Lorenz B; Litvinov D; Lee TR Light-Induced Covalent Immobilization of Monolayers of Magnetic Nanoparticles on Hydrogen-Terminated Silicon. ACS Appl. Mater, Interfaces 2010, 2, 2789–2796. [PubMed: 20857939]

(118). Khatri OP; Ichii T; Murase K; Sugimura H UV Induced Covalent Assembly of Gold Nanoparticles in Linear Patterns on Oxide Free Silicon Surface. J. Mater. Chem 2012, 22, 16546–16551.

(119). van Geel R; Pruijn GJM; van Delft FL; Boelens WC Preventing Thiol-Yne Addition Improves the Specificity of Strain-Promoted Azide–Alkyne Cycloaddition. Bioconjugate Chem 2012, 23, 392–398.

(120). L. Feldheim D; D. Keating C. Self-Assembly of Single Electron Transistors and Related Devices. Chem. Soc. Rev 1998, 27, 1–12.

(121). Wang Y; Zheng R; Ding Y; Fan W; Liu D; Zhou J; Shi J Resolving the Bond Angle of a Plasmonic Metamolecule. Optica 2017, 4, 1092–1097.

(122). Juan ML; Righini M; Quidant R Plasmon Nano-Optical Tweezers. Nat. Photonics 2011, 5, 349.

(123). Violi IL; Gargiulo J; von Bilderling C; Cortés E; Stefani FD Light-Induced Polarization-Directed Growth of Optically Printed Gold Nanoparticles. Nano Lett 2016, 16, 6529–6533. [PubMed: 27648741]

(124). Do J; Sediq KN; Deasy K; Coles DM; Rodríguez-Fernández J; Feldmann J; Lidzey DG Photonic Crystal Nanocavities Containing Plasmonic Nanoparticles Assembled Using a Laser-Printing Technique. Adv. Opt. Mater 2013, 1, 946–951.

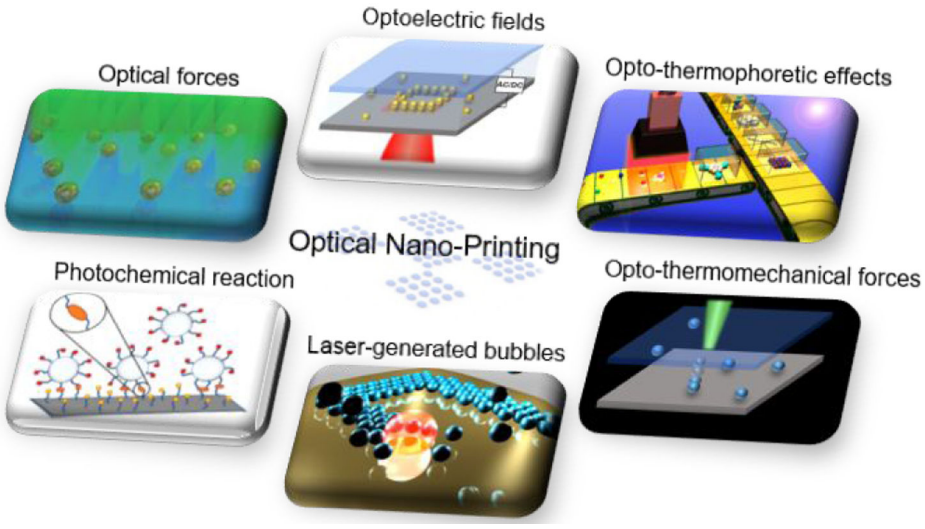


**Figure 1. Schematic illustration of optical nano-printing techniques with different physical mechanisms.**

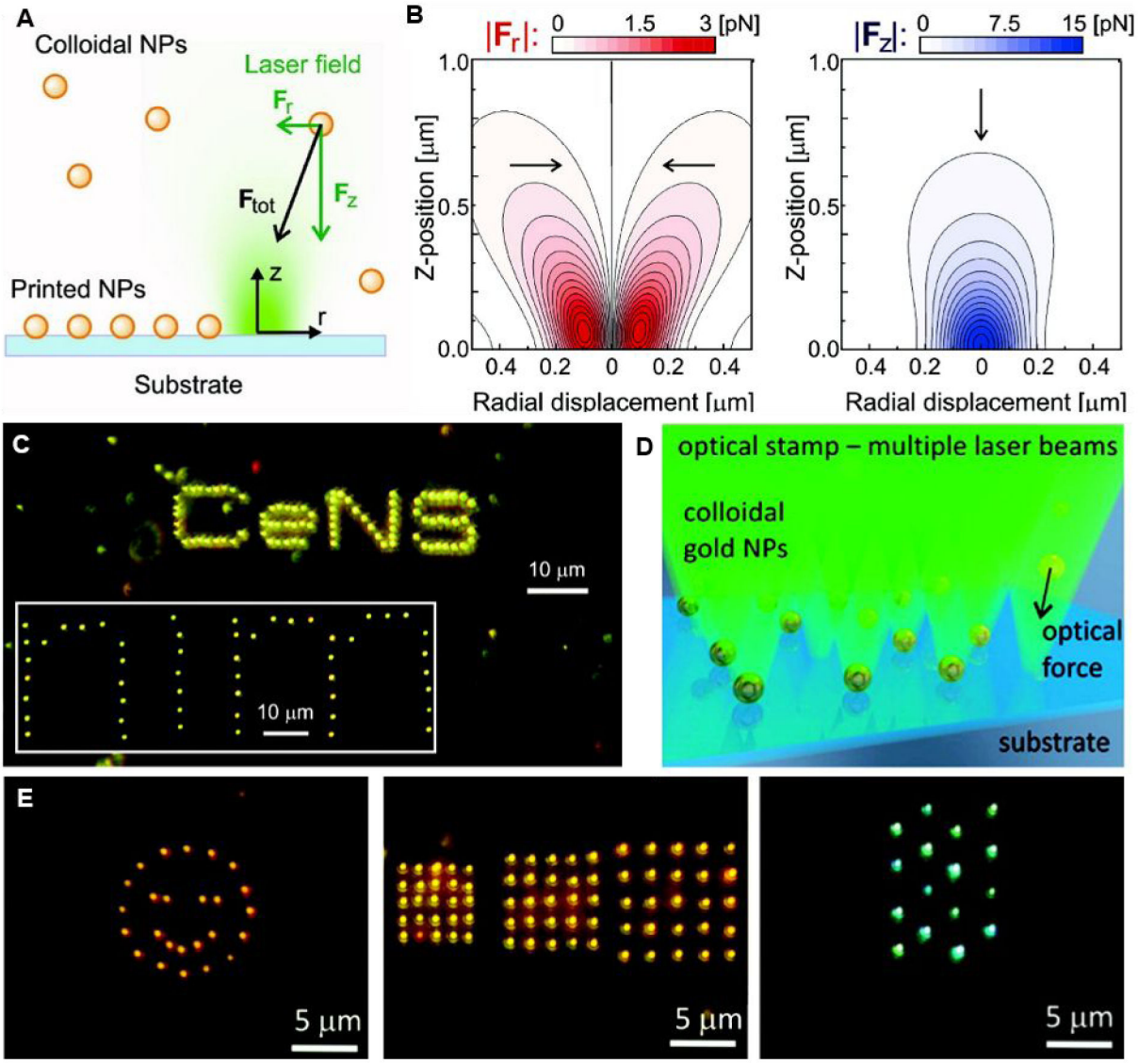


**Figure 2. Plasmon-enhanced laser printing of plasmonic nanoparticles.**

(A) Schematic illustration of the printing process and optical forces. (B) Calculated radial (left) and axial (right) optical forces on an 80 nm AuNP as a function of the position in a Gaussian focused beam. (C) A dark-field image of two patterns made by printing single AuNPs. (D) Schematic of the optical force stamping process. (E) Different stamped patterns composed of 80 nm gold or silver nanoparticles. (A-C) Adapted with permission from ref.[14] Copyright 2010, American Chemical Society. (D and E) Adapted with permission from ref. [53] Copyright 2011, American Chemical Society.

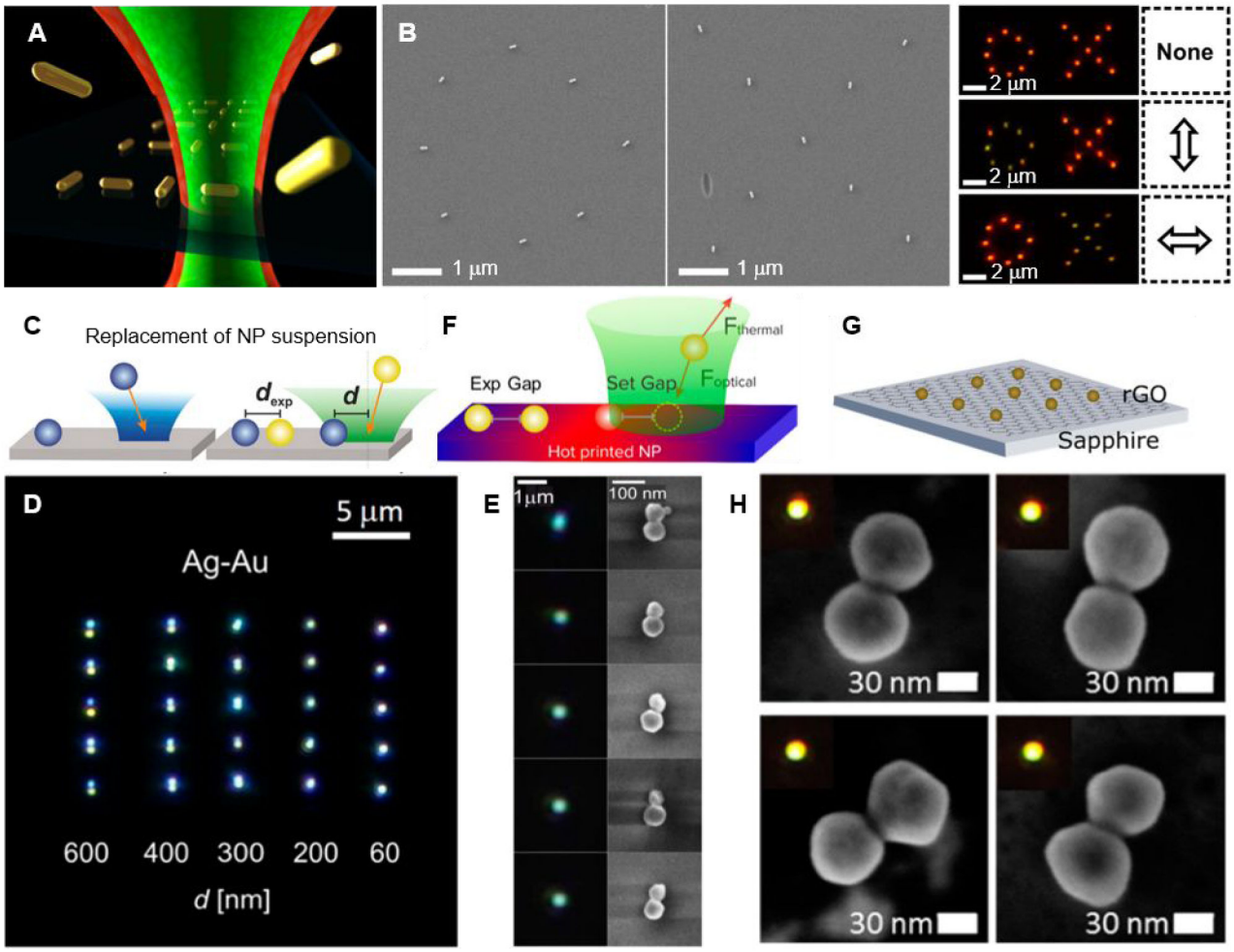


**Figure 3. Orientation control and dimer fabrication by laser printing.**

(A) Schematic illustration of two-color laser printing. (B) SEM images and polarization-dependent dark-field images of an "OX" pattern of printed AuNRs with perpendicular orientations. (C) Schematic of the process for Ag-Au heterodimer fabrication. (D) Dark-field micrographs of Ag-Au dimers fabricated at different interparticle distances *d*. (E) Dark-field (left) and field-emission SEM (right) images of fabricated Ag-Au heterodimers. (F) Schematic of the Au-Au dimer printing experiment and its relevant parameters and forces. (G) Schematic of an optically printed grid of AuNPs on a sapphire substrate coated with reduced graphene oxide. (H) Optically printed Au-Au dimers on reduced graphene oxide. (A and B) Adapted with permission from ref.[55] Copyright 2013, American Chemical Society. (C-E) Adapted with permission from ref.[57] Copyright 2016, American Chemical Society. (F-H) Adapted with permission from ref. [58] Copyright 2017, American Chemical Society.

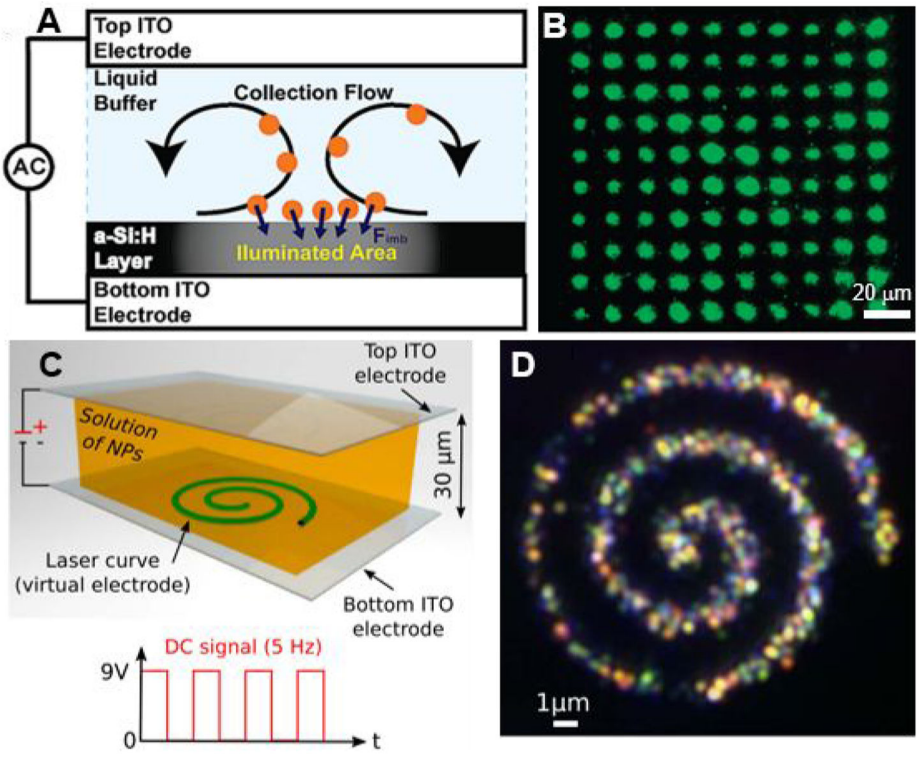


**Figure 4. Optoelectronic printing.**

(A) Optoelectronic tweezers optofluidic platform used to realize the NanoPen process. (B) Large-area patterning of 90 nm AuNPs using NanoPen in the form of a 10 × 10 array. (C) Schematic showing the setup of optoelectric printing. (D) Dark-filed image of AgNPs assemblies created along an Archimedean spiral circuit. (A and B) Adapted with permission from ref.[74] Copyright 2009, American Chemical Society. (C and D) Adapted with permission from ref.[77] Copyright 2017, Springer Nature.

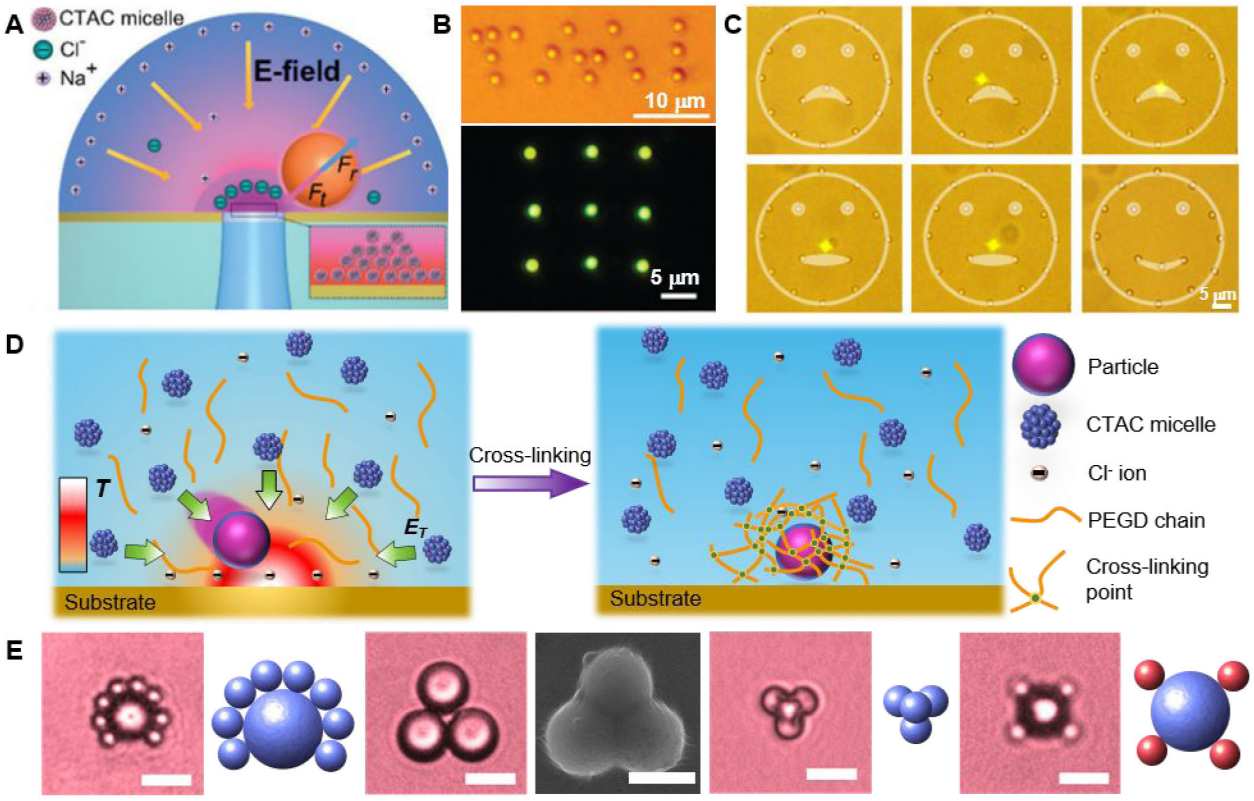


**Figure 5. Opto-thermophoretic printing.**

(A) Schematic illustration of opto-thermoelectric trapping. (B) Printed "TMI" pattern of 1 μm PS beads and 3-by-3 array of 500 nm PS beads. (C) Releasing and reprinting of a targeted colloidal particle. (D) Opto-thermophoretic construction of colloidal superstructures in photocurable hydrogels: trapping of a colloidal particle in a thermoelectric field and immobilization of the trapped colloidal particle through UV cross-linking. (E) Opto-thermophoretic assembly and patterning of various colloidal superstructures. Scale bars, 5 μm. (A-C) Adapted with permission from ref.[87] Copyright 2017, The Royal Society of Chemistry. (D and E) Adapted with permission from ref.[89] Copyright 2018, American Chemical Society.

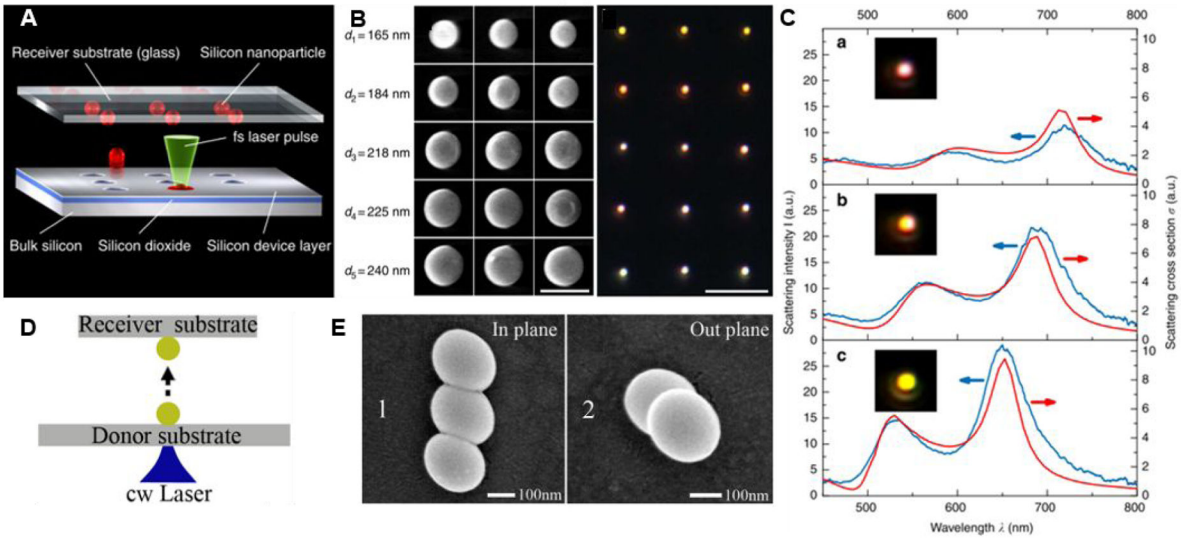


**Figure 6. Opto-thermomechanical printing.**

(A) Schematic of femtosecond laser printing of silicon nanoparticles by laser-induced transfer. (B) SEM images (scale bar, 300 nm) and dark-field microscopic images (scale bar, 5 μm) of silicon nanoparticles fabricated at different laser pulse energies. (C) Scattering spectra of silicon nanoparticles with (a) an amorphous phase, (b) a mixed phase, and (c) a crystalline phase. (D) Schematic of the release-and-place strategy. (E) SEM images of the fabricated in-plane gold nanotrimer and out-plane gold nanodimer. (A-C) Adapted with permission from ref.[93] Copyright 2014, Springer Nature. (D and E) Adapted with permission from ref.[95] Copyright 2018, American Chemical Society.

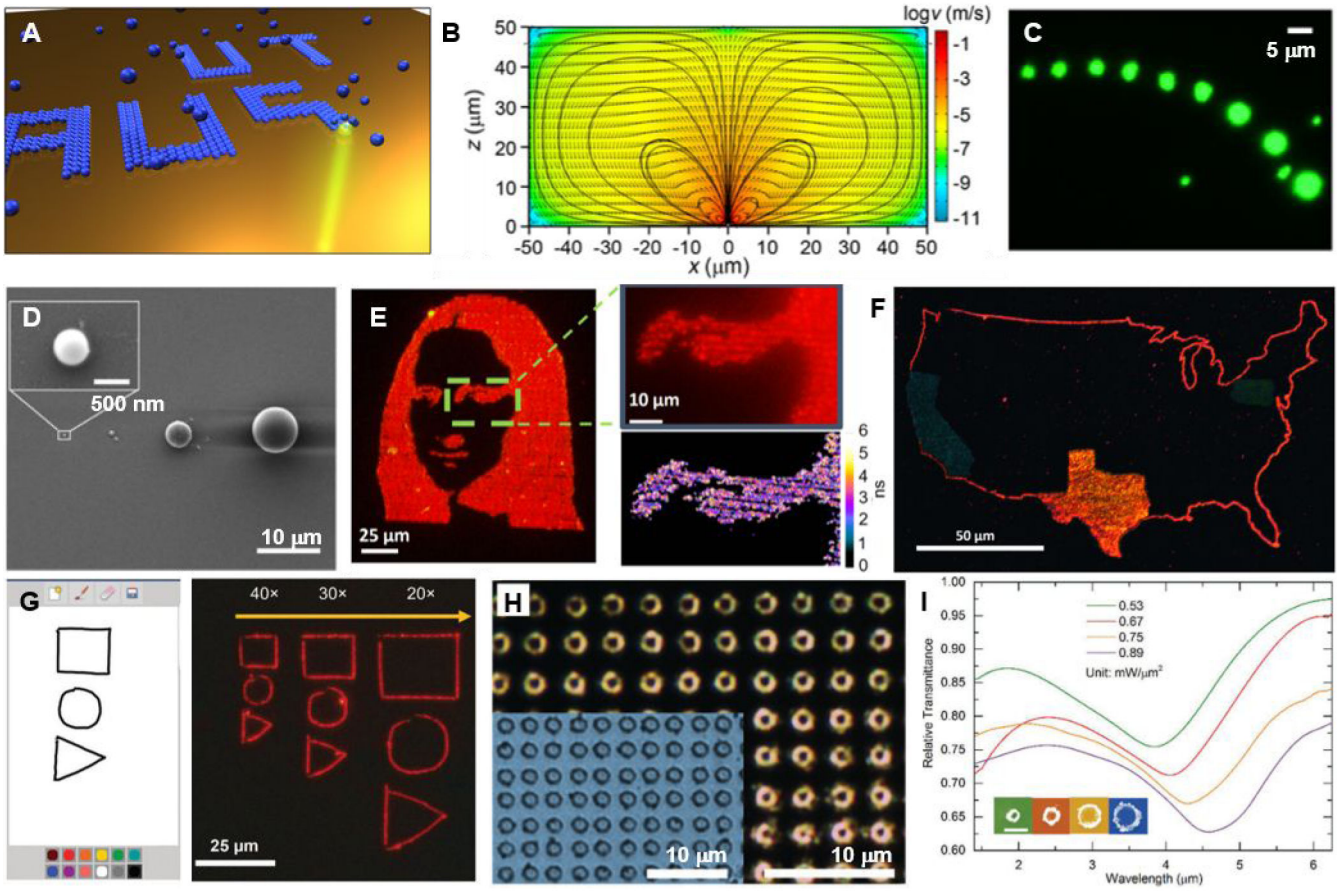


**Figure 7. Bubble printing of colloidal particles and nanostructures.**

(A) Schematic illustration of BPL. (B) Simulated Marangoni convection around a 1 μm bubble. (C) Dark-field optical image of a series of patterned 540 nm PS beads with increasing power densities. (D) Bubble printing of single particles with different sizes ranging from 540 nm to 9.51 μm. (E) “Mona Lisa” pattern of QDs with fluorescence lifetime mapping. (F) A U.S. map with the states of Texas, California, and Pennsylvania printed with different QDs. (G) Haptic interface for bubble printing at different downscaling factors. (H) Dark-field and bright-field optical image of an Ag ring array fabricated by BPL. (I) The relative transmittance spectra of the arrays of Ag rings fabricated at different laser powers. (A-D) Adapted with permission from ref.[102] Copyright 2016, American Chemical Society. (E and F) Adapted with permission from ref.[103] Copyright 2017, American Chemical Society. (G) Adapted with permission from ref.[104] Copyright 2017, The Royal Society of Chemistry. (H and I) Adapted with permission from ref.[105] Copyright 2018, Wiley-VCH Verlag GmbH & Co. KGaA, Weinheim.

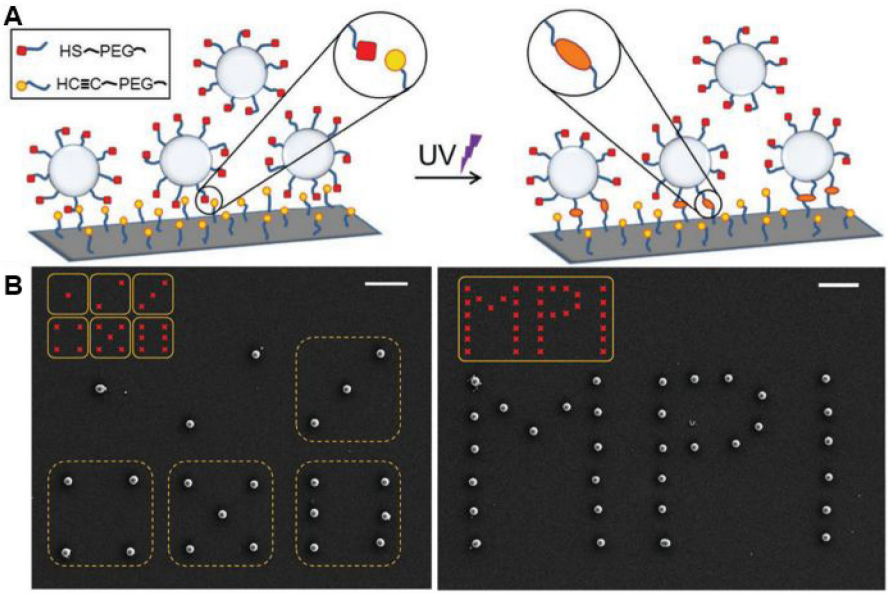


**Figure 8. Optical printing with click chemistry.**

(A) Schematic representation of the UV-induced thiol-yne reaction and its use to immobilize particles on surfaces. (B) Microstructures obtained by immobilizing 1 μm PEG-SH-functionalized silica particle assemblies by UV irradiation. Scale bars, 5 μm. Adapted with permission from ref.[43] Copyright 2016, Wiley-VCH Verlag GmbH & Co. KGaA, Weinheim.

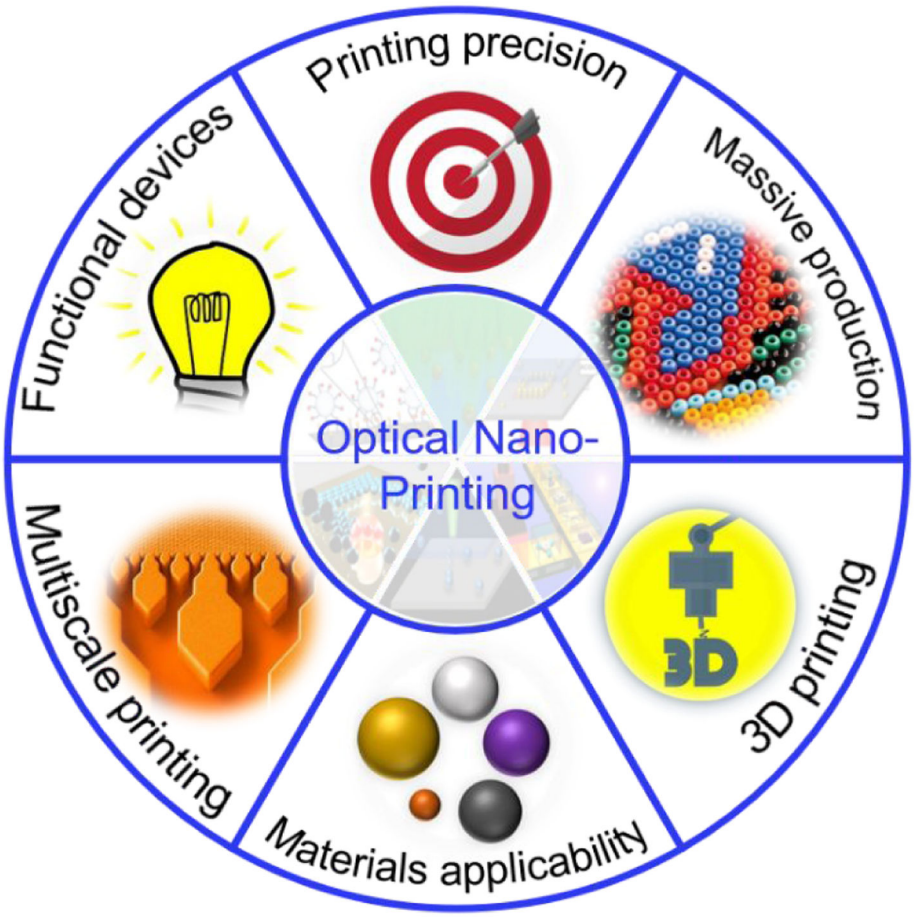


**Figure 9. Challenges and prospects for the future development of optical nano-printing.**